

# Extensions and Application of the Robust Shared Response Model to Electroencephalography Data for Enhancing Brain-Computer Interface Systems

Andrew J. Graves      Cory Clayton      Joon Yuhl Soh      Gabe Yohe      Per B. Sederberg  
*School of Data Science*   *School of Data Science*   *School of Data Science*   *School of Data Science*   *Department of Psychology*  
*University of Virginia*   *University of Virginia*   *University of Virginia*   *University of Virginia*   *University of Virginia*  
 Charlottesville, VA      Charlottesville, VA      Charlottesville, VA      Charlottesville, VA      Charlottesville, VA  
 ajg3eh@virginia.edu      acc2ds@virginia.edu      js8hh@virginia.edu      gjy7kb@virginia.edu      pbs5u@virginia.edu

**Abstract**—Brain Computer Interfaces (BCI) decode electroencephalography (EEG) data collected from the human brain to predict subsequent behavior. While this technology has promising applications, successfully implementing a model is challenging. The typical BCI control application requires many hours of training data from each individual to make predictions of intended activity specific to that individual. Moreover, there are individual differences in the organization of brain activity and low signal-to-noise ratios in noninvasive measurement techniques such as EEG. There is a fundamental bias-variance trade-off between developing a single model for all human brains vs. an individual model for each specific human brain. The Robust Shared Response Model (RSRM) attempts to resolve this trade-off by leveraging both the homogeneity and heterogeneity of brain signals across people. RSRM extracts components that are common and shared across individual brains, while simultaneously learning unique representations between individual brains. By learning a latent shared space in conjunction with subject-specific representations, RSRM tends to result in better predictive performance on functional magnetic resonance imaging (fMRI) data relative to other common dimension reduction techniques. To our knowledge, we are the first research team attempting to expand the domain of RSRM by applying this technique to controlled experimental EEG data in a BCI setting. Using the openly available Motor Movement/ Imagery dataset, the decoding accuracy of RSRM exceeded models whose input was reduced by Principal Component Analysis (PCA), Independent Component Analysis (ICA), and subject-specific PCA. The results of our experiments suggest that RSRM can recover distributed latent brain signals and improve decoding accuracy of BCI tasks when dimension reduction is implemented as a feature engineering step. Future directions of this work include augmenting state-of-the-art BCI with efficient reduced representations extracted by RSRM. This could enhance the utility of BCI technology in the real world. Furthermore, RSRM could have wide-ranging applications across other machine-learning applications that require classification of naturalistic data using reduced representations.

**Index Terms**—Brain-computer interface, Electroencephalography, Machine learning

## I. INTRODUCTION

Brain Computer Interfaces (BCI) have garnered a lot of attention in the worlds of technology, data science, medicine, and neuroscience [14, 15]. Many recent strides in BCI technology have led to astonishing new possibilities in brain research

and development [10]. A critical function of any BCI system is the ability to decode data collected from the human brain to predict subsequent behavior, which can be used for prosthetics and epilepsy research [5, 1]. Successfully deploying a model that predicts human behavior from data generated by the brain is difficult to do well, given it requires both computational speed and high accuracy. The typical BCI application requires many hours of training data from each individual to make accurate predictions specific to that individual. Moreover, there are individual differences in the organization of brain activity and low signal-to-noise ratios in noninvasive measurement techniques such as EEG.

Even though individuals have different spatial topographies with respect to brain activation, a common analytical assumption in neuroscience research is that all spatial features are anatomically aligned. This assumption imposes a structure such that all brain activation across individuals operates in a similar location in space [4]. This assumption extends beyond anatomical alignment into temporal dynamics and synthetically engineered features. However, averaging topographies across subjects has not shown much promise in accuracy for training individual models [13]. To account for this limitation, a different approach is to align features based on “function” rather than space [8]. We would like to have a method that can map different functional topographies from individuals into a common shared latent space. The shared response modeling framework was designed to accomplish this task of achieving proper functional alignment across individuals [3].

### A. Prior work on shared response modeling

The Robust Shared Response Model (RSRM) is a latent variable model that projects a collection of time series into a compressed feature space [13]. In order to learn representations common between brains under a specific task protocol, RSRM extracts components that are shared across individuals. RSRM and its close variants [Shared Response Model (SRM)] were initially developed for applications with functional magnetic resonance imaging (fMRI) data under tasks that involve temporally synchronized naturalistic stimuli [3, 11]. SRM

demonstrated superior performance on applications to fMRI data over other common dimension-reduction methods such as Principal Component Analysis (PCA) and Independent Component Analysis (ICA). RSRM was able to successfully extract both common features between subjects and unique features within subjects despite different functional topographies in the raw data space [13]. The key difference between RSRM and SRM is that SRM only maps to a shared feature space, and does not directly model individual differences. Experimental results for RSRM in comparison to the SRM showed that the RSRM performed slightly better than the SRM as well as trained faster in time segment matching and classification [13].

Notably, there does not seem to be any prior work applying the shared response modeling framework to domains outside of fMRI. This paper presents new experiments that suggest RSRM is a useful dimension reduction technique in the context of decoding brain signals using EEG. We have reason to hypothesize that directly modeling individual differences using RSRM instead of SRM could lead to better performance in EEG environments. The aim of this paper is to investigate the utility of RSRM for EEG interfaced movement control applications. We will begin with a brief mathematical description of RSRM. Then we will describe simulations to demonstrate recovery of latent time-series signals using RSRM. Finally, we will discuss our empirical application of RSRM to model EEG data.

## II. METHODS

### A. RSRM notation and formulation

Let  $N$  be the number of subjects,  $v$  the number of features,  $k$  the number of latent components, and  $t$  the number of events. The following expression is the primary equation for the RSRM [13] (see Figure 1 for the model design as applied to EEG).

$$\mathbf{X}^{(i)} = \mathbf{W}^{(i)}\mathbf{R} + \mathbf{S}^{(i)} + \mathbf{E}^{(i)}, \quad i = 1 \dots N \quad (1)$$

where  $(i)$  is the indexer for each individual subject and

- $\mathbf{X}^{(i)} \in \mathbb{R}^{v_i \times t}$  is the data matrix.
- $\mathbf{W}^{(i)} \in \mathbb{R}^{v_i \times k}$  is the matrix mapping from the observed subject space to the shared latent space.
- $\mathbf{R} \in \mathbb{R}^{k \times t}$  is the shared-response matrix.
- $\mathbf{S}^{(i)} \in \mathbb{R}^{v_i \times t}$  is the non-shared matrix unique to each individual subject.
- $\mathbf{E}^{(i)} \in \mathbb{R}^{v_i \times t}$  is an additive noise matrix specific for each subject.

Equation (1) is then estimated by solving the following optimization problem:

$$\min_{\mathbf{S}^{(i)}, \mathbf{W}^{(i)}, \mathbf{R}} \sum_{i=1}^N \frac{1}{2} \|\mathbf{X}^{(i)} - \mathbf{W}^{(i)}\mathbf{R} - \mathbf{S}^{(i)}\|_F^2 + \lambda_i \|\mathbf{S}^{(i)}\|_1 \quad (2)$$

s.t.

$$\mathbf{W}^{(i)T} \mathbf{W}^{(i)} = \mathbf{I}, \quad \forall i = 1 \dots N.$$

Equation (2) is a non-convex optimization problem, but we can estimate subsets of the model using convex optimization techniques and then combine the results at the end. Using Block Coordinate Descent, we can partition the variables into blocks and optimize each block while fixing the other blocks constant. In RSRM, each individual mapping from the latent space  $\mathbf{W}^{(i)}$ , each individual non-shared/unique matrix  $\mathbf{S}^{(i)}$ , and the shared response model  $\mathbf{R}$  is a block. Because optimizing each of these blocks while keeping the other blocks constant is a convex problem, we can approximate the global optimum with a greedy solution. This is an iterative optimization procedure by which we apply the three following routines defining the block coordinate descent.

First, we solve for  $\mathbf{W}^{(i)}$  by using the Procrustes method [6]

$$\mathbf{W}^{(i)} = \mathbf{U}^{(i)}\mathbf{V}^{(i)T} \quad (3)$$

where  $\mathbf{U}^{(i)}\mathbf{V}^{(i)T}$  is achieved through singular value decomposition (SVD)

$$\mathbf{U}^{(i)}\mathbf{\Sigma}^{(i)}\mathbf{V}^{(i)} = (\mathbf{X}^{(i)} - \mathbf{S}^{(i)})\mathbf{R}^T. \quad (4)$$

Second, we solve for  $\mathbf{S}^{(i)}$  using a soft shrinkage penalty

$$\mathbf{S}^{(i)} = \text{Shrink}(\mathbf{X}^{(i)} - \mathbf{W}^{(i)}\mathbf{R}, \lambda) \quad (5)$$

where the amount of shrinkage is determined by  $\lambda$ . More specifically, soft shrinkage is applied to  $\mathbf{D}^{(i)} \in \mathbb{R}^{v_i \times t}$

$$s = S_{\lambda_i}(d) = \begin{cases} (|d| - \lambda_i)\text{sign}(d), & \text{if } |d| > \lambda_i \\ 0 & \text{otherwise,} \end{cases} \quad (6)$$

where the individual residual  $\mathbf{D}^{(i)}$  is

$$\mathbf{D}^{(i)} = \mathbf{X}^{(i)} - \mathbf{W}^{(i)}\mathbf{R}. \quad (7)$$

In other words, soft shrinkage of  $\mathbf{D}^{(i)}$  is equal to  $\mathbf{S}^{(i)}$ . Last, we solve for  $\mathbf{R}$  with

$$\mathbf{R} = \frac{1}{N} \sum_{i=1}^N \mathbf{W}^{(i)T} (\mathbf{X}^{(i)} - \mathbf{S}^{(i)}). \quad (8)$$

We can specify the shrinkage parameter  $\lambda$  to balance how much is shared ( $\mathbf{R}$ ) by all subjects and how much is unique to each subject ( $\mathbf{S}^{(i)}$ ). As  $\lambda \rightarrow \infty$ , the model is equivalent to the deterministic solution where  $\mathbf{S}^{(i)} \rightarrow 0$ . As  $\lambda \rightarrow 0$ , there will

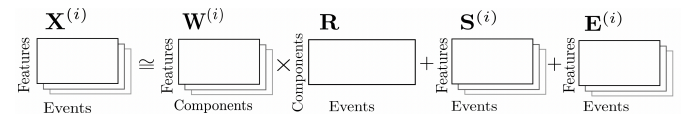


Fig. 1. Visual depiction of the matrices that represent the RSRM. For this EEG application, features are an array of time-frequency values over each channel. Components ( $k$ ) are the latent vectors extracted by RSRM. The translation of this model from fMRI to EEG data was not trivial, given their respective temporal and spatial resolution limitations. Note that dropping the additive noise matrix  $\mathbf{E}^{(i)}$  makes this an approximate solution.

be no shared response between individuals and all portions are unique to each individual ( $\mathbf{S}^{(i)} \rightarrow \mathbf{X}^{(i)}$ ). Additionally, we can specify the number of components we want our model to compute. This is analogous to selecting the number of components in PCA.

### B. Experiment 1: Simulation methods

In order to get an intuitive sense that RSSRM works for EEG-like time series, we simulated data with known parameters and attempted to recover them through visualization of the latent shared space. For this simulation, we translated the extant Python RSSRM code [9] into the R programming language, both for other R programmers to use and to check the robustness of implementations using different numerical libraries. Sine-waves with specific frequencies  $f$  are a simple surrogate for simulating EEG time-series signals. Given RSSRM is greedy and there are no guarantees that it will return the globally optimal solution, we predicted output that visually matches our prior expectation, rather than searching for a specific point estimate for  $f$ . This is because multiple signals will likely be embedded into the same latent space and will not be perfectly separated. Alternatively, one could compute a Fast Fourier transformation of the latent vector to estimate its power at specific frequencies.

The simulation incorporated signals from 32 electrodes and 100 different individuals. We randomly sampled two different deterministic sine-wave signals [10 Hz, 25 Hz] across electrodes. Different individuals had randomly sampled locations of the signals across the scalp to test if RSSRM could effectively recover signals that were not spatially aligned. We perturbed these sine-wave signals by adding Gaussian noise generated by  $N \sim (\mu = 0, \sigma = 4)$ . Let  $A$  be amplitude,  $\theta$  phase angle offset, and  $\mathbf{t} \in \mathbb{R}^N$  represent time. Sine-waves were generated with the following expression

$$A \sin(2\pi f \mathbf{t} + \theta) \quad (9)$$

fixing  $A = 1$ ,  $\theta = 0$ , and  $N = 1000$ . We attempted to recover all instances of  $f$  in the latent shared response space. We fit exactly two components to test if the two recovered latent vectors resembled the two true signal distributions. We experimentally manipulated  $\lambda$  values [0, 100000] to test its role in modeling shared latent spaces.

### C. Experiment 2: Empirical application methods

1) *Dataset description:* In order to test the application of RSSRM on our EEG data, we used the openly available EEG Motor Movement/Imagery Dataset [12]. We chose this dataset as a benchmark because it includes data from a large number of individuals (relative to other openly available EEG datasets), and the specific tasks are directly related to solving motor movement problems using BCI. This dataset contains 12 two-minute task-related runs (i.e., recordings) for each individual. Each person performed four different tasks under three separate runs. The four tasks are:

1) Open and close left vs. right fist

2) Imagine opening and closing left vs. right fist

3) Open and close both fists vs. both feet

4) Imagine opening and closing both fists vs. both feet

Each task includes two motor movements of interest with at least 21 trials for each motor movement (see Figure 2). Thus, each task allows us to make 42 predictions for each individual subject, which results in 4410 classification labels for each task.

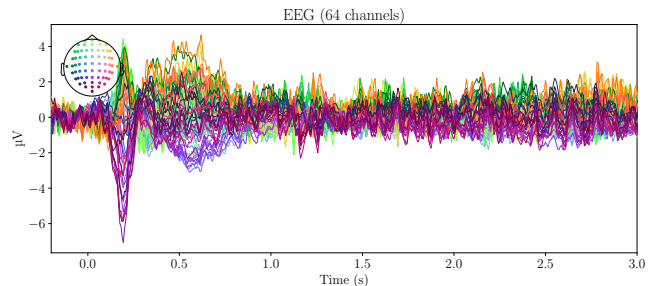


Fig. 2. Example evoked difference waveform of one of the motor movement tasks: imagining closing fists vs. imagining closing feet. The majority of the visually distinguishable signals in the time domain occur in the 200-1000 ms range and are spatially distributed across the brain.

2) *EEG Pre-processing Workflow:* The Raw EEG Motor Movement/Imagery Dataset was pre-processed using the MNE and pyprep Python software libraries [7, 2]. First, we loaded the data and added channel location coordinates. Next, we applied a band-pass filter [infinite impulse response (IIR) Butterworth model; high-pass cutoff: 1 Hz, low-pass cutoff: 50 Hz] to smooth the brain signals. Bad channels were automatically identified by low signal-to-noise ratios, near zero-variance recordings, and large deviations from nearby spatial regions. Then an average reference was applied to the data, which subtracts the average signal across the brain to improve signal-to-noise ratios across electrodes. Then we spatially interpolated all identified bad channels to preserve the dimensionality of the dataset across individuals. We segmented the data into 3 second trials with a 200 ms baseline relative to stimulus onset, which cued the individual to perform the task of interest. We then realigned the task events such that each individual had the same sequence of trial type for each task. This was necessary because fitting RSSRM requires a temporal synchronization with respect to classification labels, while EEG experiments typically randomize the onset of specific events. For the final feature engineering step, we decomposed the signals into a time-frequency representation using Morlet wavelets. From this decomposition, we generated 12 families of frequencies logarithmically spaced between 3 Hz and 45 Hz. We averaged these time-frequency representations across 400 ms time-windows strictly to keep the data input at a manageable size for our unsupervised learning experiments. We reshaped the data such that the time-frequency representations for each channel were encoded as rows of the data matrix, and the specific events were encoded as the columns of the matrix.

3) *Experimental Design*: In order to test the capacity of RSRM to effectively represent relevant brain signals in a reduced space, we systematically varied the dimensionality of the reduced space and compared decoding performance with other traditional dimension-reduction techniques. We used the BrainIAK software library in Python for fitting RSRM [9]. The unsupervised learning techniques employed were RSRM, PCA, ICA, and within-subject PCA. For RSRM, each individual had its own matrix  $\mathbf{X}^{(i)} \in \mathbb{R}^{6144 \times 42}$ , later transposed and concatenated after applying RSRM fit and transformation methods. For within-subject PCA, each individual matrix was the transpose of the initial RSRM matrices and were trained independently for each subject. For PCA and ICA, each of these individual matrices were concatenated into one single matrix  $\mathbf{X} \in \mathbb{R}^{4410 \times 6144}$ . For each model, we reduced the original feature representation into a specified number of components  $k$ . Then we trained a support vector machine classifier with a radial basis function kernel to decode one class from the other for each task. We chose not to tune the hyper-parameters  $C$  and  $\gamma$  because our primary research question concerned the relative accuracy of each dimension-reduction technique, rather than optimizing performance for each model configuration. We estimated model performance by using leave-one-run-out cross-validation. For each task, there were three runs which resulted in three folds. Thus, we trained each model on 28 events from each subject and then tested them on the remaining 14 subject events until we had predictions for all 42 events for each subject. Because of this validation scheme, we were constrained by RSRM to fit at most 28 latent components ( $k \ll v$  given that  $v = 6144$ ). For RSRM,  $\lambda$  was held constant at 2.5 and the model was run with 2 iterations. We chose a low number of iterations such that the model training time would be as short as possible.

### III. RESULTS

#### A. Experiment 1: Simulation results

Using 10 Hz and 25 Hz sine-wave signals perturbed by a stochastic distribution  $N \sim (\mu = 0, \sigma = 4)$ , we generated a raw collection of time-series signals. We fit RSRM to these raw signals to test its ability to recover the deterministic signals. We were able to capture the majority of the deterministic sine-wave distribution, which represents the true signal without noise, within two components of the RSRM given a high value of  $\lambda$  (Figure 3). This gives us confidence that this modeling procedure may prove to be useful for application in EEG.

#### B. Experiment 2: Empirical application results

After validating the potential utility of RSRM for EEG-like data structures, we compared the performance of RSRM to PCA, ICA, and within-subject PCA for classification tasks within the Motor Movement/ Imagery Dataset. We observed that RSRM demonstrated superior performance for all 4 tasks, yielding significantly higher decoding accuracy (see Figure 4 and Table I). Statistical comparisons only include RSRM in relation to within-subject PCA, because PCA and ICA performed much worse than RSRM given most values of

RSRM simulation results visualizing the primary latent space vectors

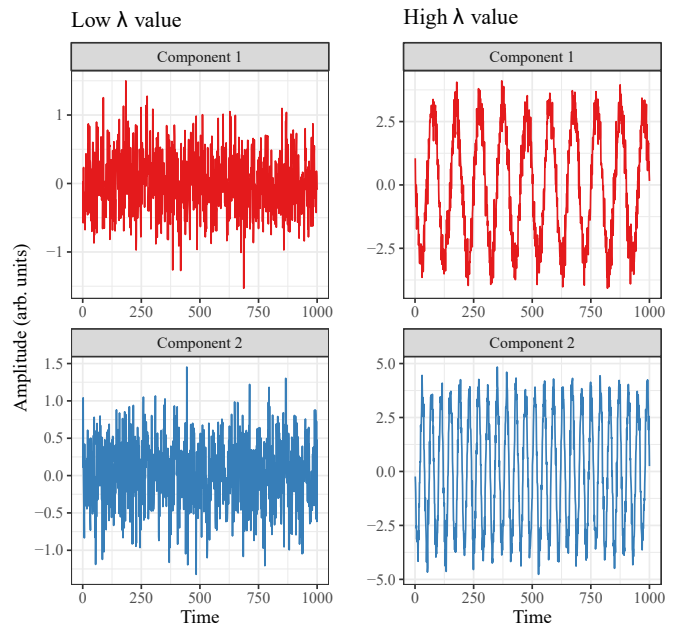


Fig. 3. First two RSRM components captured from noisy sine-wave signals. As predicted, When  $\lambda$  was very low, the model learned almost no shared information across individuals. Thus, the left side of the figure is only capturing an idiosyncratic and stochastic distribution across subjects. When  $\lambda$  is very high, the model prioritizes shared information across individuals over unique information. This is why the first two components are primarily capturing the deterministic signal in the distribution, namely 10 Hz (top-right) and 25 Hz (bottom-right). For non-simulated applications,  $\lambda$  is a hyperparameter that can be tuned to balance this trade-off.

$k$ . This pattern of results is consistent with the previous literature in fMRI [3]. This suggests that RSRM is a useful feature engineering step for EEG processing pipelines, when the dimensionality of the input space needs to be reduced.

### IV. DISCUSSION

#### A. Summary

The primary purpose of this research was to investigate whether a robust shared response model can effectively factor common and unique EEG signals between the brains of different individuals into a reduced feature space. When applied to a relatively simple machine learning classification model, the data pre-processed by RSRM was able to predict significantly above chance and was able to outperform all other dimension reduction techniques that we tested. The results suggest that RSRM captured aspects of the shared feature space above and beyond standard dimension reduction techniques typically used in neuroscience.

#### B. Limitations and Future Directions

The primary limitation of this experiment was the relatively low values of accuracy on each of the four tasks. We believe this is due to our leave-one-run-out cross-validation scheme, which constrained us to training the RSRM on only 28 events for each subject. Based on the patterns in Figure 4,

RSRM performs better on four distinct tasks relative to other dimension reduction methods

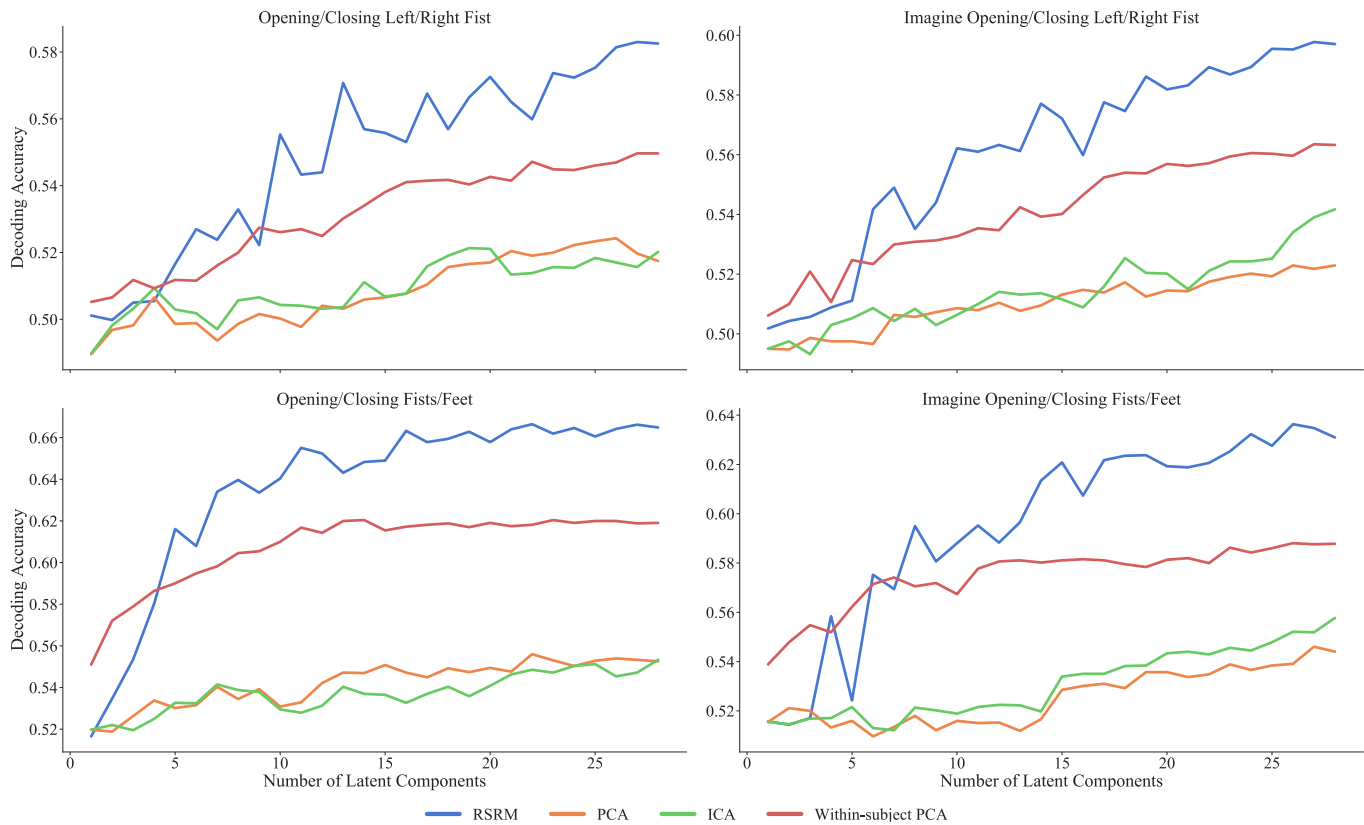


Fig. 4. Primary results from Experiment 2. RSRM outperforms on all four tasks relative to other standard dimension reduction techniques that were tested (chance decoding performance = 0.50). Here, we are analyzing relative accuracy between these methods, rather than trying to maximize accuracy with one single model configuration. The crucial accuracy difference is when the number of components is 28. Additionally, the RSRM latent representation improves performance at lower values of  $k$ . Importantly, it appears that increasing  $k$  would likely increase the differences in performance between RSRM and the other three techniques. Note that PCA and ICA require  $k \gg 28$  to reach the current performance level of RSRM from this experiment (fixing  $k = 28$  for RSRM).

TABLE I  
PAIRED  $t$ -TESTS COMPARING RSRM TO WITHIN-SUBJECT PCA ACROSS ALL NUMBER OF COMPONENTS

Task	$t$	$df$	$p$
Open and close left vs. right fist	6.73	27	< .001
Imagine opening and closing left vs. right fist	6.78	27	< .001
Open and close both fists vs. both feet	6.15	27	< .001
Imagine opening and closing both fists vs. both feet	4.05	27	< .001

the accuracy looks as though it would likely increase as additional components computed by RSRM are added. We also did not fine-tune any specific classifier for any given model configuration, as we wanted to be able to make direct comparisons across each model instance. Finally, there are likely more principled ways to feature engineer the data before fitting RSRM to EEG. For example, we averaged the Morlet wavelet decomposition time-frequency representations over 400 ms time-windows, which only provides a crude estimate and may in fact conflate multiple independent processes into one single vector.

We plan on running future experiments on different datasets with enough components for the accuracy to stabilize, in conjunction with more sophisticated feature engineering and

supervised learning. In fact, RSRM could be particularly beneficial to deep learning frameworks whose training requires large amounts of data. Applying RSRM to artificial neural networks would allow combining datasets across individuals for training. Future work will expand these experiments to predicting more than two classes, as well as attempting to decode brain signals in a streaming real-time application. Despite these stated limitations, we argue that this work contributes toward the cumulative science of designing better BCI systems.

### C. Conclusions

Training BCIs on EEG data is challenging due its relatively low signal-to-noise ratio. The typical BCI application requires building a new decoding model for each patient

due to the unique anatomical and functional topographies between patients' EEG signals. This research attempted to tackle these problems by applying RSRM, which is known to work well with fMRI data, and adapt it to function with scalp EEG data. We found that RSRM as a feature engineering step outperformed PCA, ICA, and within-subject PCA across four different motor movement tasks. A key attribute of RSRM is its ability to reduce dimensionality in the data, which leads to a significant reduction in model training time as well as a reduction in training data needed to build a sufficient model. This has the ability to have a meaningful impact on patients' lives who require a BCI for performing specific tasks. Furthermore, RSRM could have wide-ranging applications across other machine-learning applications that require decoding/classification of naturalistic data using reduced representations.

#### ACKNOWLEDGMENT

We would like to thank our project mentors Dr. Timothy W. Clark, Dr. Mohammad Sadnan Al Manir, and the UVA School of Data Science for their training, and feedback throughout this research project's development. We also would like to thank the UVA Department of Psychology for their intellectual support that made this research possible.

#### REFERENCES

- [1] Rafeed Alkawadri. "Brain-Computer Interface (BCI) Applications in Mapping of Epileptic Brain Networks Based on Intracranial-EEG: An Update". In: *Frontiers in Neuroscience* 13 (2019). Publisher: Frontiers. ISSN: 1662-453X. DOI: 10.3389/fnins.2019.00191. URL: <https://www.frontiersin.org/articles/10.3389/fnins.2019.00191/full>.
- [2] Nima Bigdely-Shamlo et al. "The PREP pipeline: standardized preprocessing for large-scale EEG analysis". In: *Frontiers in Neuroinformatics* 9 (2015). Publisher: Frontiers. ISSN: 1662-5196. DOI: 10.3389/fninf.2015.00016. URL: <https://www.frontiersin.org/articles/10.3389/fninf.2015.00016/full>.
- [3] Po-Hsuan (Cameron) Chen et al. "A Reduced-Dimension fMRI Shared Response Model". In: *Advances in Neural Information Processing Systems* 28. Ed. by C. Cortes et al. Curran Associates, Inc., 2015, pp. 460–468. URL: <http://papers.nips.cc/paper/5855-a-reduced-dimension-fmri-shared-response-model.pdf>.
- [4] Jonathan D. Cohen et al. "Computational approaches to fMRI analysis". In: *Nature Neuroscience* 20.3 (Mar. 2017). Number: 3 Publisher: Nature Publishing Group, pp. 304–313. ISSN: 1546-1726. DOI: 10.1038/nn.4499. URL: <https://www.nature.com/articles/nn.4499>.
- [5] Daniel Elstob and Emanuele Lindo Secco. "A Low Cost Eeg Based Bci Prosthetic Using Motor Imagery". In: *arXiv:1603.02869 [cs]* (Mar. 9, 2016). arXiv: 1603.02869. URL: <http://arxiv.org/abs/1603.02869>.
- [6] John C. Gower and Garmt B. Dijksterhuis. *Procrustes problems*. Vol. 30. Oxford, UK: Oxford University Press, Jan. 22, 2004. 248 pp. ISBN: 978-0-19-851058-1. URL: <http://www.oup.com/uk/catalogue/?ci=9780198510581>.
- [7] Alexandre Gramfort et al. "MEG and EEG data analysis with MNE-Python". In: *Frontiers in Neuroscience* 7 (2013). Publisher: Frontiers. ISSN: 1662-453X. DOI: 10.3389/fnins.2013.00267. URL: <https://www.frontiersin.org/articles/10.3389/fnins.2013.00267/full>.
- [8] James V Haxby et al. "Hyperalignment: Modeling shared information encoded in idiosyncratic cortical topographies". In: *eLife* 9 (June 2, 2020). Ed. by Chris I Baker and Floris P de Lange. Publisher: eLife Sciences Publications, Ltd, e56601. ISSN: 2050-084X. DOI: 10.7554/eLife.56601. URL: <https://doi.org/10.7554/eLife.56601>.
- [9] Manoj Kumar et al. "BrainIAK tutorials: User-friendly learning materials for advanced fMRI analysis". In: *PLOS Computational Biology* 16.1 (Jan. 15, 2020). Publisher: Public Library of Science, e1007549. ISSN: 1553-7358. DOI: 10.1371/journal.pcbi.1007549. URL: <https://journals.plos.org/ploscompbiol/article?id=10.1371/journal.pcbi.1007549>.
- [10] Elon Musk and NeuroLink. "An integrated brain-machine interface platform with thousands of channels". In: *J Med Internet Res* 21.10 (2019), p. 12. DOI: 10.2196/16194. URL: <http://www.jmir.org/2019/10/e16194/>.
- [11] Hugo Richard et al. "Fast shared response model for fMRI data". In: (Sept. 27, 2019). arXiv: 1909.12537 [cs.CV]. URL: <https://arxiv.org/abs/1909.12537>.
- [12] Gerwin Schalk et al. "BCI2000: a general-purpose brain-computer interface (BCI) system". In: *IEEE transactions on bio-medical engineering* 51.6 (June 2004), pp. 1034–1043. ISSN: 0018-9294. DOI: 10.1109/TBME.2004.827072.
- [13] Javier S. Turek et al. "Capturing Shared and Individual Information in fMRI Data". In: *2018 IEEE International Conference on Acoustics, Speech and Signal Processing (ICASSP)*. ICASSP 2018 - 2018 IEEE International Conference on Acoustics, Speech and Signal Processing (ICASSP). Calgary, AB: IEEE, Apr. 2018, pp. 826–830. ISBN: 978-1-5386-4658-8. DOI: 10.1109/ICASSP.2018.8462175. URL: <https://ieeexplore.ieee.org/document/8462175/>.
- [14] J. J. Vidal. "Real-time detection of brain events in EEG". In: *Proceedings of the IEEE* 65.5 (May 1977). Conference Name: Proceedings of the IEEE, pp. 633–641. ISSN: 1558-2256. DOI: 10.1109/PROC.1977.10542.
- [15] J. J. Vidal. "Toward Direct Brain-Computer Communication". In: *Annual Review of Biophysics and Bioengineering* 2.1 (1973), pp. 157–180. DOI: 10.1146/annurev.bb.02.060173.001105. URL: <https://doi.org/10.1146/annurev.bb.02.060173.001105>.